Int. J. Heat Mass Transfer. Vol. 28, No. 3, pp. 631–640, 1985
Printed in Great Britain

0017-9310/85 $3.00 + 0.00

Buoyancy in developed laminar curved tube flows

JY-BER LEE, H. A. SIMON✠ and J. C. F. CHOW*
Department of Mechanical Engineering, University of Illinois at Chicago, Illinois, U.S.A.

(*Received* 7 *February* 1984 *and in final form* 12 *September* 1984)

Abstract—The influence of buoyancy on fully developed laminar flow in curved tubes of circular cross-section is studied numerically. Steady flow for a constant property fluid, in terms of the Boussinesq approximation, is assumed. The thermal boundary conditions are specified as axially uniform heat flux and peripherally uniform wall temperature. The problem is solved using coarse, unequally spaced grids. The solutions cover a wide range of Prandtl, Dean and Grashof numbers and include the curvature ratio as an explicit parameter. The results are compared with results from the literature and reveal considerable differences. The buoyancy acts to increase the average Nusselt number, change the local Nusselt number distribution around the periphery, and rotate the orientation of the secondary flow.

1. INTRODUCTION

THE PERFORMANCE of curved tube flows, with regard to skin friction and heat transfer has been studied analytically, numerically and experimentally. For example, see refs. [1, 2, 3]. The secondary circulation in the cross-sectional plane arises because of a non-uniform pressure field induced by centrifugal forces. Fluid at the central region of a pipe has the highest axial velocity and experiences a greater centrifugal force than that near the pipe wall, where the axial velocity is lower. Two vortices are formed with the horizontal diameter as a line of symmetry [2, 4].

The parameter characterizing curved tube flow is the ratio of inertial forces to viscous forces and is known as the Dean number, $De = Re\sqrt{(a/R')}$. It should be noted that several researchers in the field [4, 5, 6], use different definitions of the Dean number, such as:

$$De' = Re_S^2(a/R')$$

or Dean's original parameter [2]

$$K = 2Re_S^2(a/R') = 2De'.$$

If a temperature distribution is present, flows can also be induced by buoyancy effects. At low Reynolds numbers, this natural convection effect is predominant in the secondary flow, depending upon the physical properties and the difference between the wall and the bulk temperatures. The varying gravitational force due to differences in density causes the motion of fluid elements in the vertical direction. If the fluid near the wall is heated, the colder, heavier fluid at the center of the pipe moves towards the bottom and the fluid at the bottom returns to the top along the tube wall. This effect forces the secondary flow into two vertical vortices, the line of symmetry being a vertical line [7].

Three definitions of the Grashof number are commonly used. The first is defined in terms of the difference between the bulk and wall temperatures $\Delta T'$, $Gr' = g\beta\Delta T'L^3/\nu^2$; the second uses the axial wall temperature gradient τ, $Gr'' = g\beta\tau L^4/\nu^2$, and the corresponding Rayleigh number is $Ra'' = Gr''Pr$; the last one uses the heat flux at the wall q'', $Gr = g\beta q''L^4/\kappa\nu^2$. In all three definitions L is a characteristic length, equal to a in this study. Thus, $Gr = Gr''RePr/4 = Ra''Re/4 = Gr'Nu/2$ for heat transfer in fully developed flow inside a tube with constant peripherally averaged heat flux at the wall.

In combination, the centrifugal and buoyancy forces generate two skewed vortices. The strength of the secondary flow is enhanced and the dividing streamline between the two vortices is inclined. The point of maximum axial velocity does not lie on the center line, but shifts towards the outer part of the tube cross-section under the influence of the centrifugally induced secondary flow. The axial velocity is also distorted by the buoyancy forces, the displacement being downwards in the case of a cold core [5, 6, 8].

The basic analytical approaches to the curved tube flow and heat transfer problem have all been severely limited. Dean's perturbation analysis [2, 4], which was the first work theoretically to predict secondary flow in curved tubes, is limited to a small curvature ratio, a/R', and very low Reynolds numbers (i.e. low Dean numbers, $De < 18$). Numerical methods [1, 9, 10, 11] have been applied to obtain the solution for higher Dean number flows, extending De up to 1,200. The agreement of the flow friction factors and heat transfer coefficients from theories, numerical solutions, and experimental measurements appear satisfactory. The effect of buoyancy has been studied by Morton [12] and Newell and Bergles [13] for straight tubes, and by Yao and Berger [6] and Prusa and Yao [5] for curved tubes with values of De equal to 177 and less. Considerable differences are found in the current work as compared with [5] and these are discussed later in the paper.

The current study is one part of a broader investigation into pulsatile flows in curved tubes. Here the effect of buoyancy is included for steady flows in

✠ The editors regret to announce the death of Professor Harold Simon on 25 September 1984.

* To whom correspondence should be addressed.

NOMENCLATURE

a tube radius
d tube diameter
f friction factor
g gravitational constant
h radial increment in modified coordinates or local heat transfer coefficient
q'' peripherally averaged constant wall heat flux
r dimensionless radial coordinate
u dimensionless radial component of velocity
v dimensionless tangential component of velocity
w dimensionless axial component of velocity
A_ζ nonlinear coefficient in equation (3), also see equation (4)
$\mathbf{B}$ vector in equation (11)
C tridiagonal coefficient matrix in equation (11)
De Dean number
De' modified Dean number
Gr modified Grashof number, $\beta g a^4 q''/\kappa\nu^2$
Gr' Grashof number $\beta g a^3 \Delta T'/\nu^2$
Gr'' modified Grashof number, $\beta g a^4 \tau/\nu^2$
I unit matrix
K modified Dean number, $2De'$
L characteristic length
Nu local Nusselt number
$\overline{Nu}$ peripherally averaged Nusselt number
P nondimensional pressure
Pe_ζ generalized Peclet number, see equations (3) and (4b)
Pr Prandtl number
R_0 dimensionless coil ratio, R_0'/a
R dimensionless toroidal radius
Ra'' modified Rayleigh number based on axial wall temperature gradient
Re Reynolds number based on averaged axial velocity and pipe diameter
Re_s Reynolds number for corresponding straight pipe
S_ζ source term in equation (3), also see equation (4)
T dimensionless temperature
T_m bulk or averaged temperature over the cross section
T_w peripherally constant wall temperature.

Greek symbols
α thermal diffusivity
β coefficient of volumetric thermal expansion
ζ dummy variable for w or T... etc.
θ angular coordinate in plane of tube curvature
κ fluid thermal conductivity
λ inertia of iteration
ν fluid kinematic viscosity
ξ dimensionless axial component of vorticity
ρ fluid density
τ axial wall temperature gradient
ϕ angular coordinate in tube cross section
Ψ dimensionless secondary stream function
ΔT the difference between the T_w and T_m
ϕ_T location of maximum heat transfer
ϕ_f location of maximum skin friction.

Superscript
' denotes dimensional variable.

Subscript
c quantity for curved pipe
s quantity for corresponding straight pipe.

curved tubes with a relatively wide range of Prandtl, Grashof and Reynolds numbers. No restrictction is placed on a/R. The results reported here are for De equal to 320 and less, and for the curvature ratio in the range $1/4 \geqslant a/R \geqslant 1/150$. In these cases, buoyancy has a significant effect on the heat transfer performance. This study reveals the influence of curvature explicitly and omits pitch effect. Thus, trends resulting from curvature ratio alone may be seen, though admitting that at large curvature ratios pitch effect is likely to be important. The inclusion of pitch effect is part of a proposed future study.

In practice, it is more reasonable to specify the wall heat flux than to specify the axial wall temperature gradient. Hence the buoyancy is introduced in terms of the heat flux Grashof number Gr. The maximum value of Gr reported here is 60,000. From the energy balance over an infinitesimal control volume, it can be shown that the parameter $ReRa''$ used by Prusa and Yao [5] is equivalent to $4Gr$ as defined here. Note, this equivalence only holds when the Re in ref. [5] is based on the average axial velocity.

2. ANALYSIS

Consider a circular tube of radius a coiled in a horizontal circle of radius R', with zero pitch, as shown in Fig. 1.

The buoyancy forces are approximated by the Boussinesq form in these equations [5, 6, 12, 13]. The range of validity of the Boussinesq approximation has been documented in [14] for the case of natural

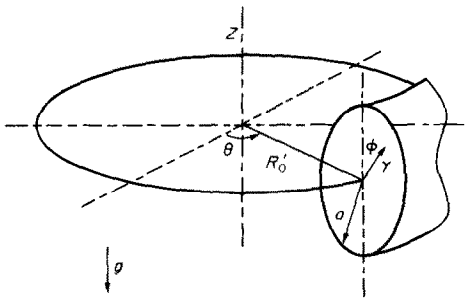

FIG. 1. Toroidal coordinate system.

convection in a horizontal fluid layer, corresponding to the Rayleigh–Benard problem.

The following nondimensional variables are introduced

$$r=\frac{r'}{a},\quad R_0=\frac{R'_0}{a},\quad R=\frac{R'}{a}\quad R=R_0+r\sin\phi$$

$$u=\frac{a}{\nu}u',\quad v=\frac{a}{\nu}v',\quad w=\frac{a}{\nu}w',\quad u=-\frac{1}{rR}\frac{\partial\Psi}{\partial\phi},$$

$$v=\frac{1}{R}\frac{\partial\Psi}{\partial r},\quad T=\frac{T'_w-T'}{4aq''}\kappa Re,\quad p=\frac{a^2P'}{\rho\nu^2},$$

$$Gr=\frac{\beta g a^4 q''}{\kappa\nu^2} \tag{1}$$

and an axial vorticity is defined as

$$\xi=\frac{1}{r}\left[\frac{\partial(rv)}{\partial r}-\frac{\partial u}{\partial\phi}\right]=\left(\frac{1}{rR}-\frac{\sin\phi}{R^2}\right)\frac{\partial\Psi}{\partial r}+\frac{1}{R}\frac{\partial^2\Psi}{\partial r^2}-\frac{\cos\phi}{rR^2}\frac{\partial\Psi}{\partial\phi}+\frac{1}{r^2R}\frac{\partial^2\Psi}{\partial\phi^2}. \tag{2}$$

The general conservation form of the dimensionless equations governing the axial vorticity ξ, axial velocity w, and temperature T for a steady, incompressible, variable temperature laminar fluid can be expressed as

$$A_\zeta\zeta+\frac{1}{rR}\frac{\partial[(rRu)\zeta]}{\partial r}+\frac{1}{rR}\frac{\partial[(Rv)\zeta]}{\partial\phi}=\frac{Re}{Pe_\zeta rR}\left[\frac{\partial}{\partial r}\left(rR\frac{\partial\zeta}{\partial r}\right)+\frac{\partial}{\partial\phi}\left(\frac{R}{r}\frac{\partial\zeta}{\partial\phi}\right)\right]+S_\zeta \tag{3}$$

where ζ is a dummy variable for ξ, w and T, and A_ξ, A_w, A_T are given by

$$A_\xi=\frac{1}{R^2}\left(1-\cos\phi\frac{\partial\Psi}{\partial r}+\frac{\sin\phi}{r}\frac{\partial\Psi}{\partial\phi}\right)$$

$$A_w=\frac{1}{R^2}\left(1+\cos\phi\frac{\partial\Psi}{\partial r}-\frac{\sin\phi}{r}\frac{\partial\Psi}{\partial\phi}\right), \tag{4a}$$

$$A_T=0.$$

Also

$$Pe_\zeta=Pe_w=Re$$

$$Pe_T=PrRe. \tag{4b}$$

The following terms are referred to as source terms

$$S_\xi=2\frac{w}{R}\left(\cos\phi\frac{\partial w}{\partial r}-\frac{\sin\phi}{r}\frac{\partial w}{\partial\phi}\right)+\frac{4Gr}{Re}\left(\frac{\cos\phi}{r}\frac{\partial T}{\partial\phi}+\sin\phi\frac{\partial T}{\partial r}\right)$$

$$S_w=-\frac{1}{R}\frac{\partial p}{\partial\theta}\qquad S_T=w\frac{R_0}{R}. \tag{4c}$$

The boundary conditions are: no-slip condition on the wall, axially uniform heat flux, peripherally uniform wall temperature, and the value of the stream function on the wall is assigned to zero. The boundary condition for the vorticity can be derived from equation (3).

$$\left.\begin{aligned} w=T=\Psi=0\\ \xi=\frac{1}{R}\frac{\partial^2\Psi}{\partial r^2}\end{aligned}\right\}\qquad \text{when}\quad r=1. \tag{5}$$

An expression for the local Nusselt number can be found by considering the following expression for the local heat flux at the wall

$$q=\kappa(\partial T'/\partial r')_{r'=a}=h(T'_w-T'_m). \tag{6}$$

In terms of the dimensionless temperature, equation (6) can be expressed as

$$Nu=\frac{2ha}{k}=\frac{-2(\partial T/\partial r)_{r=1}}{T_m}. \tag{7}$$

An expression for the peripherally averaged Nusselt number can be found by considering the overall heat balance

$$q''=\bar{h}(T'_w-T'_m) \tag{8}$$

substituting this into the definition of the dimensionless temperature T gives

$$\overline{Nu}=\frac{Re}{2T_m} \tag{9}$$

where T_m is the nondimensional bulk temperature over the flow cross section and is defined by

$$T_m=\frac{2}{\pi Re}\int_0^{2\pi}\int_0^1 wTr\,dr\,d\phi. \tag{10}$$

3. NUMERICAL METHOD

The radial gradients of the dependent variables are always higher near the wall than in the core region. Hence the governing equations are discretized into a set of finite difference equations, using a non-uniform grid spacing. The grid intervals are smaller closer to the wall than in the core region. A 15 × 32 grid system, on the full circle, is used.

The central point of the tube cross section $r=0$ is a singular point. Terms such as $(1/r)\,\partial\Psi/\partial r$ require special treatment, and terms like $\partial\Psi/\partial\theta$ become undefined at this point. The latter difficulty is avoided if the axis of symmetry exists, but this is often not the case. There are several papers dealing with the singular point problem

[1, 5, 10, 15, 16]. The singularity problem can be eliminated simply by not locating a mesh point at the origin in this problem. The central point of the cross-section of the tube is of no special physical significance, and nothing is lost by omitting it from the set of mesh points, see Fig. 2.

The finite difference form adopted uses a hybrid scheme as discussed by Patankar [17].

The hybrid scheme is used not only because of the numerical stability concern, but also because it simulates the physical mechanism more closely. The variations of ζ are of exponential type and far from being linear except for small values of Pe_ζ. When Pe_ζ is large, the value of ζ at the midpoint of two grid points is nearly equal to the value of ζ at the upstream point. The central difference scheme is not accurate in this condition, unless a much finer grid system is assigned, leading to increased computational time. The upwind scheme proposed in the literature [18] has two major shortcomings:

1. 'Upwind-assignment' is only good for large Pe_ζ, not for all Pe_ζ. For small Pe_ζ the central difference scheme is more reasonable.

2. When Pe_ζ is large, the diffusion term is nearly zero at the midpoint. The upwind scheme always calculates the diffusion term from a linear profile assumption, and thus overestimates diffusion at large values of Pe_ζ.

The application of the hybrid scheme used here can be understood by observing that:

1. It is identical with the central difference scheme when the Peclet number is small.

2. When the Peclet number is large, it reduces to the upwind scheme in which the diffusion term has been set equal to zero.

The four governing equations (3) and (4a), (4b) and (4c) are coupled and highly nonlinear (except for the stream function equation). If the semi-implicit method, e.g. alternating direction implicit (ADI) method, is used, the finite difference equations corresponding to equations (4a), (4b) and (4c) form a set of equations of the form

$$C^i\zeta^{i+1} = \mathbf{B}^i \tag{11}$$

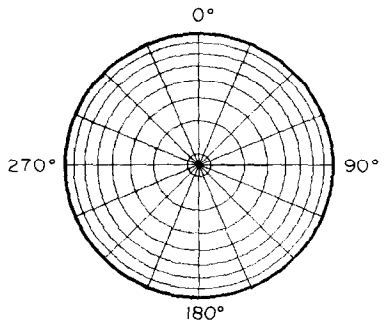

FIG. 2. Representation of variable grid spacing.

where ζ denotes the dependent variables w, ξ, and T. C is a tridiagonal matrix and is a function of the stream function Ψ, the coordinates and the grid spacings; $\mathbf{B}$ is a vector and is a function of Ψ, ζ, and the source term Q. The superscript i indicates the iteration number.

A numerical investigation of the coefficient matrix C shows that it is not diagonally dominant. This leads to instability in the numerical solution. Akiyama and Cheng [9] experienced similar difficulty and suggested the use of a finer mesh. This entails longer computation time, and consequently larger round-off errors. On the other hand, a mixed method combining the ADI and, Successive Under-Relaxation (SUR), method has been used by a number of researchers [11]. In this method, the inertial λ [19], is introduced such that the matrix C becomes diagonally dominant. This removes the numerical instability and, in addition, functions as an under-relaxation factor. Unfortunately, the inertia λ is very difficult to determine, and usually it takes many test runs to find a suitable value, so there is not much overall improvement in computation time. Consequently, the point by point method, i.e. SUR, is used here. Convergent results are always easily found by choosing a suitable relaxation factor. The relaxation factor for the stream function equation is always chosen as 1.2, because this equation is linear. The relaxation factors of the other equations are always between 0.5 and 0.9. It should be noted that if an under-relaxation factor that is too small is used, convergence may be slowed considerably. In this case the usual type of convergence check may, in fact, lead to erroneous conclusions.

The residual of a dependent variable in each control volume as given by Patankar [17] is used here: convergence is assumed when the residual is less than 10^{-4}. This normally requires on the order of 100 major iterations. A spatial-convergence check was performed by comparing almost all results with solutions using a 9×16 grid point mesh. A maximum change of only 1.5% in the global Nusselt number and axial friction factor was detected. A few cases using a 31×64 grid were carried out and showed a 0.3% change over the 15×32 grid used here. The considerable increase in computer time was not felt to be warranted.

Another check on the accuracy of the numerical solution can be made. Averaging equation (7) and comparing with equation (9) yields the following result:

$$\overline{Nu} = \frac{-1}{\pi R_0 T_m} \int_0^{2\pi} \left(\frac{\partial T}{\partial r}\right)_{r=1} R \, d\phi \tag{12}$$

and

$$\overline{Nu} = \frac{Re}{2T_m}.$$

These equations give two very different means of calculating the average Nusselt number from the numerical data. The percentage difference in the two estimates of averaged Nusselt number is taken as a measure of the error of the numerical solution. For all

runs, the maximum percentage difference between the results predicted by equation (12) is less than 1.5%. All average Nusslet number results reported here are based on the second of the equations (12).

4. RESULTS AND DISCUSSION

Among numerous numerical solutions concerning heated curved-pipe flow, only a few papers [10, 11, 19] consider the effect of finite curvature ratio. The results presented here agree well with those papers for $Gr = 0$. For the zero buoyancy case Fig. 3 compares the present results for the friction factor ratio as a function of De, with Collins and Dennis [1] and Austin and Seader [20]. The results show good agreement. Tarbell *et al.* [19] found that De alone is not sufficient to characterize the flow field and heat transfer completely. However, if the Dean number and Grashof number are held essentially constant while the curvature ratio is reduced drastically, the nature of the secondary flow is altered only slightly, as can be observed in Fig. 4. Thus the effect of the curvature ratio is accounted for mainly in the Dean number, but it does have an additional, though only slight effect, on the local friction factors and Nusselt numbers. Seventeen contours are used in all the stream function and temperature plots, and the difference between two adjacent contours, $\Delta\Psi$ or ΔT, is fixed in each case. These contour plots are very useful for visualizing the effects that various parameters have on the flow field and temperature. For example, as can be shown from equation (2), the secondary velocity is of the order (Ψ/R). High values of $(\Delta\Psi/R)$ between neighboring contour lines represents more intense secondary flows.

The highest Dean number presented here is 320. This upper value is fixed by the Boussinesq approximation, rather than numerical difficulty. For Dean numbers greater than 320, the buoyancy effect will only be important when Gr is of the order 10^6. But this requires a large $\Delta T'$ or q'', making the Boussinesq approximation unreasonable.

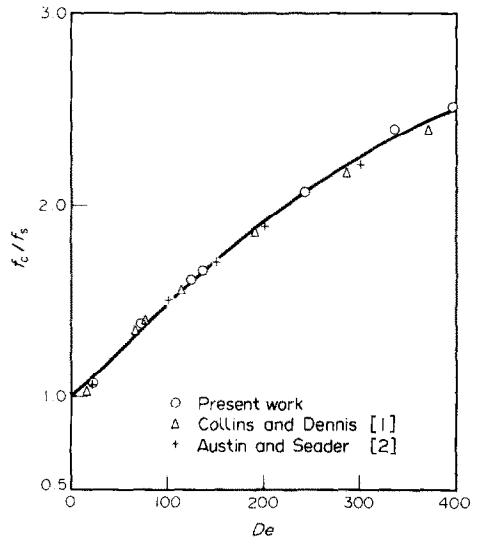

FIG. 3. Friction factor ratio compared with the literature.

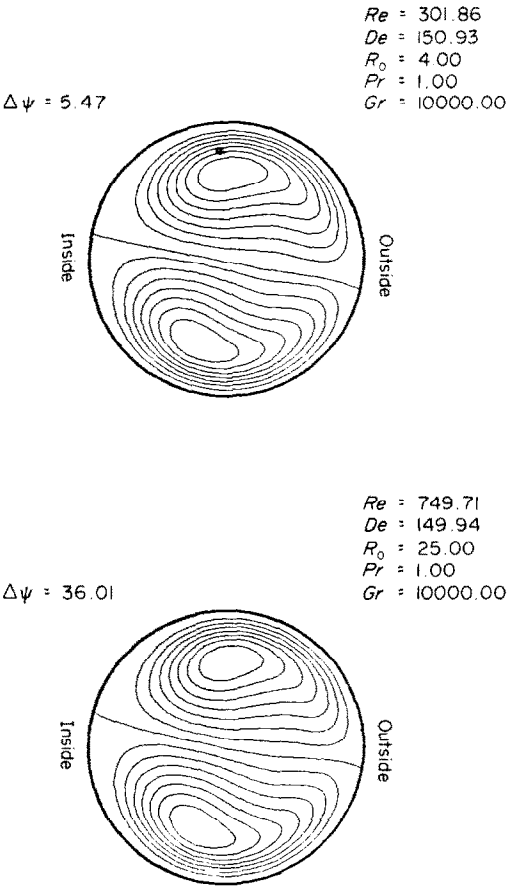

FIG. 4. Stream function contours for different curvature ratios and for Dean number approximately equal to 150.

The highest modified Grashof number Gr reported here is 60,000. For gases at room temperature, $\beta g/\nu^2$ is about 10^8 ($K^{-1}\ m^{-3}$), and κ is about 10^{-2} ($W\ K^{-1}\ m^{-1}$). If the tube radius is 0.1 m, then the wall heat flux is less than 0.1 $W\ m^{-2}$ with $Gr = 10^5$. Hence, the Boussinesq form is a valid approximation for all cases reported here, with a reasonable counterpart in practice.

The heat transfer rate is enhanced by the secondary flow and is larger than would be expected without the buoyancy effect, or without the curvature effect, given the same axial pressure gradient. This is shown in Fig. 5, where Nu_c/Nu_s is the ratio of the Nusselt number for a curved and a corresponding straight pipe, for varying values of De and Gr. This arises because the buoyancy acts to increase the magnitude of the secondary flow beyond that which is expected from centrifugal force alone. For a given Gr, as De increases, the flow becomes increasingly dominated by the centrifugal force. For this reason, the curves of constant Gr approach the lowest, or base curve for $Gr = 0$, asymptotically as $De \to \infty$. In this regime, the influence of buoyancy is

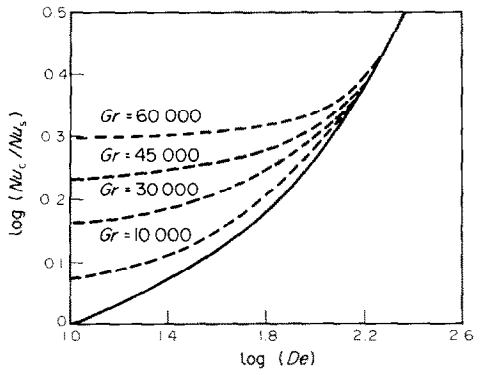

FIG. 5. Nusselt number ratio as function of Grashof and Dean numbers.

unimportant and the momentum and energy equations may be considered to be uncoupled.

Figures 6 and 7 show the axial skin friction factors and Nusselt numbers distributed around the periphery compared with the corresponding straight pipe flow. Note that Re_s, the Reynolds number that would be attained in a straight tube for the same axial pressure gradient, is shown in both figures. This is done because as the Grashof number is increased, the flow rate (and Re) decreases under the same axial pressure gradient, and a fixed Dean number cannot be obtained for different Grashof number cases.

In Figs. 6 and 7, the Dean number is approximately equal to 70. The friction factor has a higher value at the outer wall due to the higher axial velocity gradient at this location. The local heat transfer rate increases near the outer wall where the local secondary flow is similar to a stagnation point flow. Near the inner wall, the heat

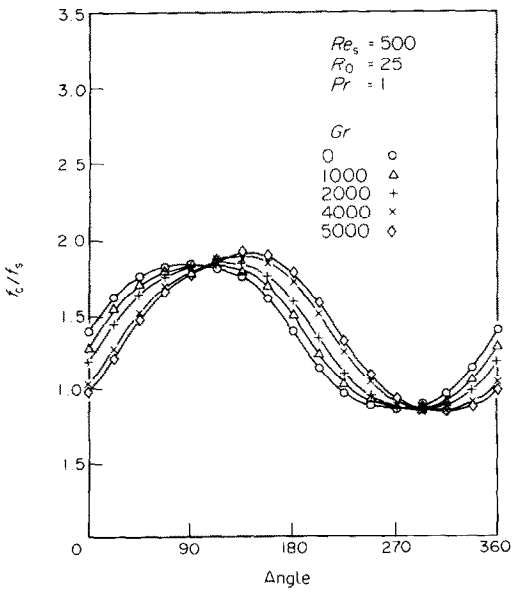

FIG. 6. Local friction factor ratio as function of Grashof number for Dean number approximately equal to 70.

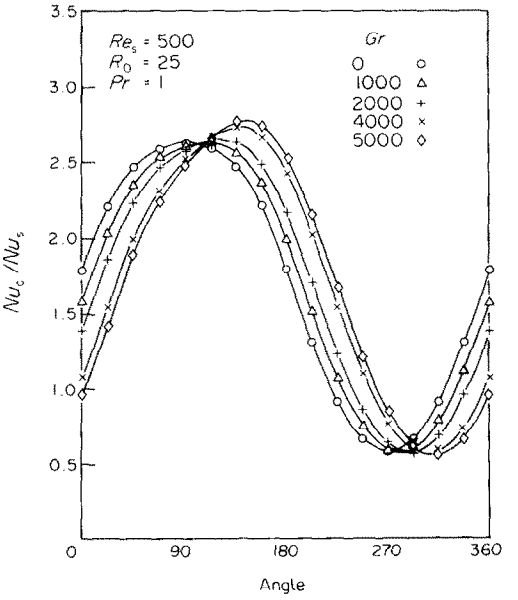

FIG. 7. Local Nusselt number ratio as function of Grashof number for Dean number approximately equal to 70.

transfer rate is a local minimum due to the reversed stagnation point flow.

Comparing Figs. 6 and 7, it is clear thar the Nusselt number ratio increases more than the skin friction factor ratio. In both figures, the maximum values are moved toward the 180° point as Gr increases.

Figure 8 shows how the Grashof number effect skews the line separating the two vortices while $\Delta\Psi/R$, an indication of the intensity of the secondary flow is increased. The dividing streamline ($\psi = 0$) is no longer a straight line in these cases. Obviously, for $De \simeq 15$ and $Gr \simeq 1200$, the secondary flow is already dominated by natural convection effects.

The influence of the secondary flows on heat transfer is more important at high Prandtl numbers in laminar flow. This is due to the more important role convection plays relative to conduction as the Prandtl number increases, leading to a reduced wall temperature for the same heat flux. Figure 9 illustrates the effect of Prandtl number on the isotherms. For low Pr the isotherms are close to concentric circles as in the straight pipe case, showing that the secondary, or transverse convection, has little effect. At high Pr the transverse convection is dominant and thin thermal boundary layers are evident on the pipe walls. The affected layer remains coherent as it returns along the diameter. It is for this reason that the effect of buoyancy is reduced, as Prandtl number increases, because far less fluid undergoes a relative density change.

The present paper shows considerable differences in detail with Prusa and Yao [5], even though the overall results are similar. This is best exemplified by examining the location on the periphery of the maximum skin friction and heat flux. Figure 9 in reference [5] compares their results with that of an

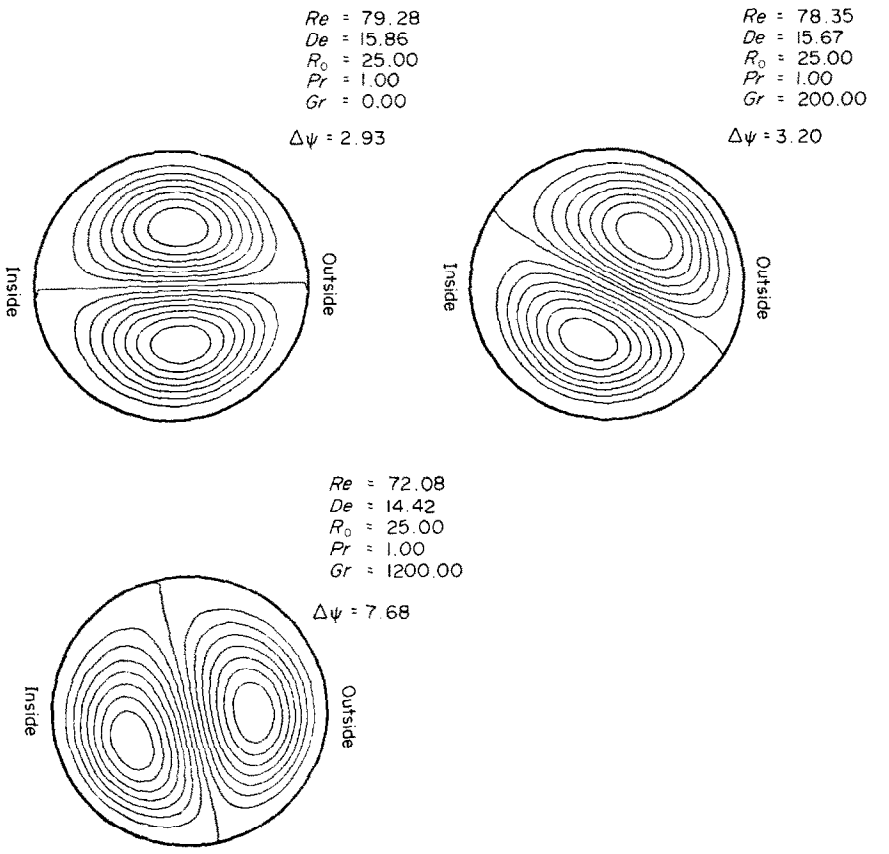

FIG. 8. Influence of Grashof number on stream function contours.

earlier paper by Yao and Berger [6] which uses a perturbation approach. In the ranges illustrated, the two sets of results differ only by a few percent, and at worst by less than 10%. The perturbation results of Yao and Berger [6], for location of the maxima, are given in closed form, permitting a direct comparison with the results of the current work. Hence, this permits an indirect comparison with the results of reference [5]. This is shown in Fig. 10, with the angular location on the periphery defined as in Figs. 1 and 2. The difference is seen to be large for $De' = 128$ for the range shown in ref. [5].

It should be noted in comparing reference [5] with the present work that the definitions of the Dean number are different. The Dean number given in Fig. 10 is that used by Prusa and Yao [5] and is defined in terms of the straight-pipe Reynolds number achieved for the same pressure gradient.

The current analysis is formulated so that the only limit on the curvature ratio is geometrical. However in reference [5], $(R_0 + r\sin\phi)$ has been replaced by R_0, limiting their solution to cases for $a/R_0 \ll 1$.

Furthermore, Chang [21] and Simon [22] examine the validity of a perturbation expansion in terms of De' and conclude that the same equations are obtained for a double expansion in terms of a/R and $1/Re_s^2$. Hence both a/R and $1/Re_s^2$ must be small for the perturbation analysis as used, for example by Yao and Berger [6], to be applicable. Dean [2] and Van Dyke [23] come to the same conclusion. It would appear from this that the results of ref. [6] should be limited to large Re. However, buoyancy effects are important when Re is small, and so there appears to be a basic question with regard to the applicability of the results obtained in ref. [5]. This could account for some of the differences observed between the current work and ref. [5].

In passing, it should also be noted that Prusa and Yao [5] give an erroneous impression, that heat transfer rate decreases as the Dean number increases. This is of course only true if the axial temperature gradient is fixed, in which case the heat transfer ratio parallels the mass flow and hence the skin friction ratio.

It is of primary concern to know the conditions for which buoyancy is dominant or can be neglected. Figure 11 shows a (Gr, De) plane which is seen to be separated into three distinct regions. In region I, the centrifugal force dominates. Here the problem can be solved by considering the momentum and energy equations are uncoupled. In region III, the buoyancy force dominates. The heat transfer can be treated here as that for a straight tube with natural convection. In the middle region II, both kinds of forces are important, and the full, coupled equations (3) and (4) have to be solved simultaneously. The limits of the forced and free

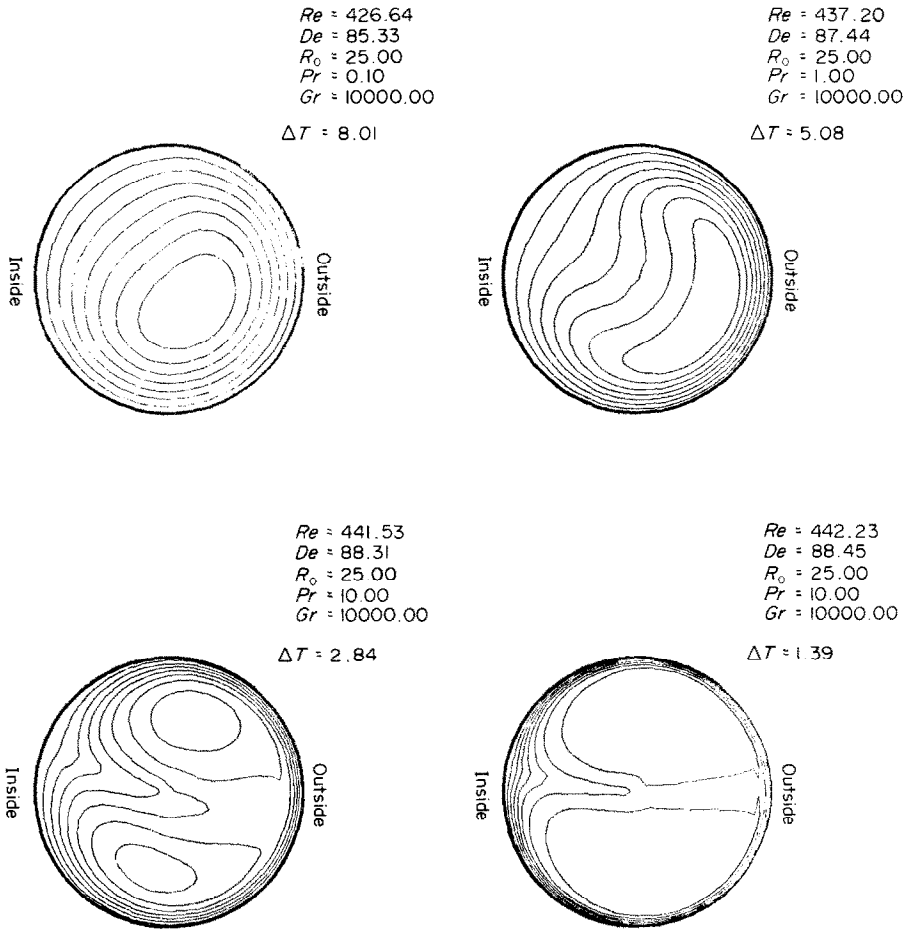

FIG. 9. Influence of Prandtl number on temperature contours.

convection regimes are defined in such a way that the actual peripherally averaged Nusselt number under the combined influence of the forces does not deviate by more than 5% from the peripherally averaged Nusselt number caused by the centrifugal forces alone or by the buoyancy forces alone.

An order-of-magnitude analysis of the equations (3) indicates a general criterion for determining whether or

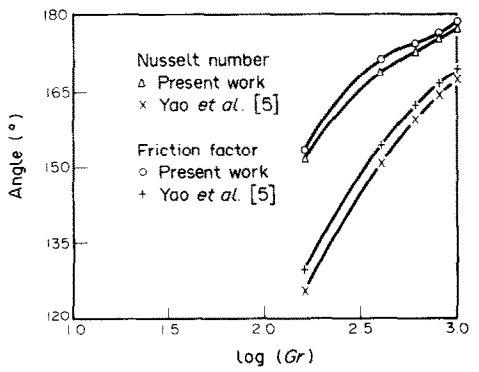

FIG. 10. Comparison of Nusselt number and friction factor maxima with ref. [6] for $De' = 128$ and $Pr = 1$.

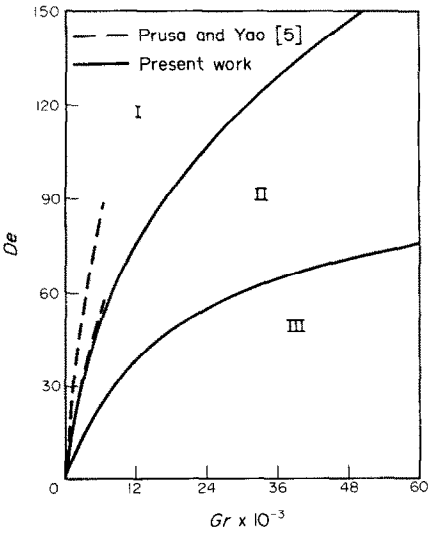

FIG. 11. Regimes of influence: (I) centrifugal force dominates; (II) both centrifugal and buoyancy forces are important; (III) buoyancy force dominates.

not natural convection effects dominate. When $Gr/De^2 > 1.0$ free convection is of primary importance. This result is in agreement with Fig. 11. Again considerable differences with ref. [5] are evident.

5. CONCLUSIONS

1. Large values of either the Gr or De can cause intense secondary circulations with marked effects on heat transfer and skin friction. The curvature ratio in the range 4–50, has a negligible explicit influence on the average Nusselt number and skin friction factor, though it has a fairly large effect on the location of the maxima.

2. A plot is given showing the relative importance of the buoyancy and centrifugal effects.

3. The results are directly applicable to mass transfer, in the absence of chemical reaction, and with ordinary diffusion, by changing the Gr to a corresponding mass diffusion Grashof number.

Acknowledgement—Support by the National Science Foundation grant CME-7919873 is gratefully acknowledged. Computational services were provided by the Computer Center of the University of Illinois at Chicago.

REFERENCES

1. W. M. Collins and S. C. R. Dennis, The steady motion of a viscous fluid in a curved tube, *Q. J. Mech. appl. Math.* **28,** 133–156 (1975).
2. W. R. Dean, The stream-line motion of fluid in a curved pipe, *Phil. Mag.* **5,** 673–695 (1928).
3. C. M. White, Stream-line flow through a curved pipe, *Proc. R. Soc.* **123A,** 645–663 (1929).
4. W. R. Dean, Note on the motion of fluid in a curved pipe, *Phil. Mag.* **4,** 208 (1927).
5. J. Prusa and L. S. Yao, Heat transfer of fully developed flow in curved tubes, ASME Publication, Paper No. 81-HT-39 (1981).
6. L. S. Yao and S. A. Berger, Flow in heated curved pipes, *J. Fluid Mech.* **88,** 339–354, 1978.
7. S. T. McComas and E. R. G. Eckert, Combined free and forced convection in a horizontal circular tube, *J. Heat Transfer* **88,** 147–153 (1966).
8. M. A. Abul-Hamayel and K. J. Bell, Heat transfer in helically-coiled tubes with laminar flow, ASME Publication, Paper No. 79-WA/HT-11 (1980).
9. M. Akiyama and K. C. Cheng, Boundary vorticity method for laminar forced convection heat transfer in curved pipes, *Int. J. Heat Mass Transfer* **14,** 1659–1675 (1971).
10. C. E. Kalb and J. D. Seader, Heat and mass transfer phenomena for viscous flow in curved circular tubes, *Int. J. Heat Mass Transfer* **15,** 801–817 (1972).
11. N. J. Rabadi, J. C. F. Chow and H. A. Simon, An efficient numerical procedure for the solution of laminar flow and heat transfer in coiled tubes, *Num. Heat Transfer* **2,** 279–289 (1979).
12. B. R. Morton, Laminar convection in a uniformly heated horizontal pipe at low Rayleigh numbers, *Q. Jl Mech. appl. Math.* **12,** 410–420 (1959).
13. P. H. Newell, Jr. and A. E. Bergles, Analysis of combined free and forced convection for fully developed laminar flow in horizontal tubes, *J. Heat Transfer* **92,** 83–93 (1970).
14. D. D. Gray and A. Giorgini, The validity of the Boussinesq approximation for liquids and gases, *Int. J. Heat Mass Transfer* **19,** 545–551 (1976).
15. R. J. Kee and A. A. McKillop, A numerical method for predicting natural convection in horizontal cylinders with asymmetric boundary conditions, *Comput. Fluids.* **5,** 1–14 (1977).
16. R. J. Kee, A numerical study of natural convection inside horizontal cylinders with asymmetric boundary conditions, Ph.D. thesis, University of California, Davis, California (1974).
17. S. V. Patankar, *Numerical Heat Transfer and Fluid Flow.* McGraw-Hill, New York (1980).
18. R. Courant, E. Isaacson and M. Rees, On the solution of non-linear hyperbolic differential equations by finite differences, *Communs pure appl. Math* **5,** 243–255 (1952).
19. J. M. Tarbell and M. R. Samuels, Momentum and heat transfer in helical coils, *Chem. Engng* **5,** 117–127 (1973).
20. L. R. Austin and J. D. Seader, Fully developed viscous flow in coiled circular pipes, *A.I.ChE. Jl.* **19,** 85–94 (1973).
21. M. H. Chang, Curved tube heat transfer in laminar, pulsatile, fully developed flows, Ph.D. thesis, University of Illinois at Chicago (1976).
22. H. A. Simon, M. H. Chang and J. C. F. Chow, Heat transfer in curved tubes with pulsatile, fully developed, laminar flows, *ASME J. Heat Transfer* **99,** 590–595 (1977).
23. M. Van Dyke, Extended Stokes series: laminar flow through a loosely coiled pipe, *J. Fluid Mech.* **88,** 129–145 (1978).

EFFET DE GRAVITE SUR LES ECOULEMENTS LAMINAIRES ETABLIS DANS LES TUBES COURBES

Résumé—On étudie numériquement l'influence de la gravité sur l'écoulement laminaire établi dans les tubes courbes à section droite circulaire. On suppose un écoulement permanent à propriétés de fluide constantes et l'approximation de Boussinesq. Les conditions aux limites thermiques sont celles de flux uniforme axialement et de température pariétale uniforme sur la circonférence. On résout le problème en utilisant des grilles inégalement espacées. Les solutions couvrent un large comaine de nombres de Prandtl, Dean et Grashof et elles incluent le rapport de courbure comme un paramètre explicite. Les résultats sont comparés avec ceux tirés de la littérature et on constate des différences considérables. La gravité agit dans le sens d'un accroissement du nombre de Nusselt moyen, d'un changement du nombre de Nusselt local sur la périphérie et d'une rotation de l'orientation de l'écoulement secondaire.

AUFTRIEB IN AUSGEBILDETEN LAMINARSTRÖMUNGEN IN GEKRÜMMTEN ROHREN

Zusammenfassung—Der Einfluß des Auftriebs auf eine voll ausgebildete laminare Strömung in gekrümmten Rohren mit runder Querschnittsfläche wird numerisch untersucht. Es wird eine stationäre Strömung mit konstanten Stoffwerten in der Form der Boussinesq-Approximation angenommen. Für die thermischen Randbedingungen werden einheitliche Wärmestromdichte in axialer Richtung und einheitliche Wandtemperatur am Umfang gewählt. Das Problem wird mit Hilfe eines groben, räumlich ungleichförmigen Gitternetzes gelöst. Die Lösungen gelten für einen weiten Bereich der Prandtl-, Dean- und Grashof-Zahl und schließen das Krümmungsverhältnis als einen expliziten Parameter mit ein. Die Ergebnisse werden mit Daten aus der Literatur verglichen und weisen beträchtliche Unterschiede auf. Der Auftrieb vergrößert die mittlere Nusselt-Zahl, verändert die Verteilung der örtlichen Nusselt-Zahl am Umfang und verdreht die Orientierung der Sekundärströmung.

ВЛИЯНИЕ МАССОВОЙ СИЛЫ НА РАЗВИТОЕ ЛАМИНАРНОЕ ТЕЧЕНИЕ В КРИВОЛИНЕЙНЫХ ТРУБАХ

Аннотация—Представлен численный анализ влияния массовой силы на полностью развитое ламинарное течение в криволинейных трубах круглого сечения. В приближении Буссинеска рассмотрено установившееся течение жидкости с постоянными свойствами. Тепловые граничные условия определены в виде однородного по оси теплового потока и однородной температуры стенки. Задача решается с использованием грубой неравномерной сетки. Решения охватывают широкий диапазон чисел Прандтля, Дина и Грасгофа и включают в качестве явного параметра отношение кривизн. Результаты сравниваются с данными, представленными в литературе, и показывают существенное различие. Подъемная сила приводит к увеличению среднего числа Нуссельта, изменяет распределение локального числа Нуссельта и меняет направление вторичного течения.